Journal of Magnetism and Magnetic Materials 654 (2026) 174171

Contents lists available at ScienceDirect

Journal of Magnetism and Magnetic Materials

journal homepage: www.elsevier.com/locate/jmmm

Research article

Oscillating topological charge for skyrmion-based spin-transfer torque nano-oscillator

Vinko Sršan [a,b,*], Matej Komelj [a,c], Sašo Šturm [a,b,d]

[a] Department for Nanostructured Materials, Jožef Stefan Institute, Jamova cesta 39, SI 1000 Ljubljana, Slovenia
[b] Jožef Stefan International Postgraduate School, Jamova cesta 39, SI 1000 Ljubljana, Slovenia
[c] Faculty of Mathematics and Physics, University of Ljubljana, 1000 Ljubljana, Slovenia
[d] Department of Geology, Faculty of Natural Sciences and Engineering, University of Ljubljana, Aškerčeva cesta 12, SI 1000 Ljubljana, Slovenia

ARTICLE INFO

Keywords:
Magnetic skyrmions
Spin torque nano-oscillator
Micromagnetics

ABSTRACT

Magnetic skyrmions are considered as promising candidates for next generation information carriers. In cubic chiral magnets with bulk Dzyaloshinskii–Moriya interaction, skyrmions trivially extend into the third dimension forming so-called skyrmion string. The third dimension of skyrmion strings introduces an additional degree of freedom that can be utilized in skyrmion-based applications. An example of such application is spin-torque oscillator based on skyrmion breathing, gyrotropic motion and skyrmion deformation mechanisms. Expanding these mechanisms, we propose design of spin-torque oscillator based on topological charge oscillation in confined geometry where skyrmion string breathing, gyrotropic motion and skyrmion-edge interactions are coupled. Micromagnetic calculations were employed to demonstrate topological charge oscillation as a function of model geometries. It is shown that only a small subset of material geometries is suitable to obtain topological charge oscillations, indicating that precise engineering of geometry would be required to realize such a device. Findings presented in this work contribute to a better understanding of a skyrmion string dynamical phenomena, which offer additional route in designing spin-torque oscillators.

1. Introduction

Magnetic skyrmions are topologically-non-trivial, vortex-like magnetization configurations. Due to a high stability, magnetic skyrmions are considered as candidates for the new generation of spintronic memory and logic devices. Their promise lies in the fact that skyrmions are characterized by topological invariant often called a topological charge or winding number defined as

$$Q = \frac{1}{4\pi}\int \vec{m}\cdot\left(\frac{\partial\vec{m}}{\partial x}\times\frac{\partial\vec{m}}{\partial y}\right)dx\,dy, \tag{1}$$

where $\vec{m} \equiv \frac{\vec{M}(x,y)}{M_s}$ represents the magnetization-direction unit vector [1]. Topological protection signifies higher order of stability, since a topologically protected object may only be annihilated by a discontinuous transformation. Magnetic skyrmions are considered topological objects since they are homotopic identity to the vector field on the unit sphere, which differentiates them from uniform states. In practice, topological protection introduces an energy barrier that separates skyrmion state from uniform (topologically trivial) state. In terms of topological charge, a state with $Q = 0$ is topologically trivial, while skyrmions are characterized by $Q = \pm 1$ [1]. It was theoretically proposed that skyrmions in materials could exist as single objects, or they could form an ordered lattice phase [2,3]. First experimental observations of magnetic skyrmions were done on cubic chiral magnets MnSi and FeGe [4,5]. Later, magnetic skyrmions were realized in multilayer thin films by depositing magnetic thin film on a layer with high spin–orbit coupling, inducing Dzyaloshinskii–Moriya interaction (DMI) at the interface of two layers [6–9]. Skyrmions are, in principle, seen as 2D objects, but in chiral bulk materials they trivially extend in third dimension forming a skyrmion string [10]. Magnetic skyrmions are considered as future energy efficient spintronic devices because they exhibit unique static and rich dynamical properties [11–16] Until recently, application possibilities were mainly assessed using two-dimensional skyrmions, but presence of the skyrmion extension into third dimension offers additional degree of freedom that could be utilized since skyrmion strings could be further manipulated along their length [17–19]. While driven by external forces like applied field, electric current or temperature gradient, skyrmion strings can be twisted, bent, branched or annihilated by a topological-defect mediation [20–23]. Among many targeted applications of magnetic skyrmions, significant focus has been dedicated towards the design of skyrmion based spin-torque oscillators (STO) that

* Corresponding author at: Department for Nanostructured Materials, Jožef Stefan Institute, Jamova cesta 39, SI 1000 Ljubljana, Slovenia.
E-mail address: vinko.srsan@ijs.si (V. Sršan).

https://doi.org/10.1016/j.jmmm.2026.174171
Received 5 November 2025; Received in revised form 28 February 2026; Accepted 27 April 2026
Available online 18 May 2026

can be utilized for future applications in neuromorphic computing as physical artificial neurons, microwave-frequency generators and many more [24–30]. Thus far, main mechanisms involved in the STO design include gyrotropic motion of the skyrmion in the disc, skyrmion breathing and periodic skyrmion deformation [28,30–32]. The gyrotropic motion assumes skyrmion motion along circular or spiral trajectories in nanodots or constrained geometries. Skyrmion breathing represents periodic radial contraction and expansion without skyrmion motion. Typical frequencies generated by the skyrmion gyration and breathing are in the GHz range. Deformation modes utilize skyrmion shape deformation as a frequency generation mechanism, which allows usage of various device geometries. As of now, skyrmion gyration, breathing, and deformation are promising mechanisms for frequency generation with good tunability potential and device simplicity in spite of several limitations being present. Mainly, frequency stability is highly dependent on the presence of defects and interaction of skyrmion with the edge of the nanostructure. Additionally, skyrmion collision with device edges can lead to annihilation at stronger current driving, therefore limiting frequency tunability with arbitrarily strong electrical currents.

It is noted that device shape can play an important role in skyrmion oscillation and skyrmion stability. Therefore in this work, we utilize the geometry of a device for the emergence of the additional oscillation mode that is based on topological charge unwinding. In particular, we aim to utilize skyrmion string dynamics under applied electrical current drive due to their intrinsic features like bending and resistance to annihilation upon contact with the device edge. To this end, we explore electrical current-driven dynamics of skyrmion strings in highly confined geometries, where skyrmion tube diameter is a small fraction of lateral material dimensions, by means of computational micromagnetism. Skyrmion strings were stabilized in geometries with circular and rectangular cross-sectioned materials with a varied width and thickness. Current driven dynamics was studied in precessional regime with ultra-low Gilbert damping. Our results demonstrate an existence of a window, defined by of material dimensions and applied current densities that accommodate the presence of topological charge oscillation, that can be utilized as a mechanism for designing skyrmion string-based spin-torque oscillators.

2. Methods

We consider a skyrmion-hosting chiral magnetic system with bulk DMI. In particular, we focus on creating a model which accommodates its spatial dimension as a function of the helical length, which is one of the detrimental factors for skyrmion stability, dynamics and size. Three-dimensional (3D) objects hosting the magnetic skyrmion strings have been considered for distinct models differentiated by their geometric shapes, namely a square prism and a cylinder, which from here on will be called a nanorod and a nanowire, respectively. The widths of nanorods (w) and diameters of nanowires (d) were set to 35, 45 and 55 nm, allowing us to analyse skyrmion string dynamics for different ratios of skyrmion string diameter (D_{sky}) and lateral dimension of the models (d, w). Lastly, skyrmion stability and dynamics are influenced by the material thickness, which dependence was studied by setting the length (t) of nanorods and nanowires to be 25, 50, 75 and 100 nm [33]. A scheme of the modelled geometries is depicted in Fig. 1.

Total energy of the system is given as:

$$E = -A\vec{m}\nabla^2\vec{m} + D\vec{m}(\nabla \times \vec{m}) - \frac{1}{2}\mu_0 M_s \vec{m}\cdot\vec{H}_d - \mu_0 M_s \vec{m}\cdot\vec{H}, \quad (2)$$

where A, D, μ_0, M_s, H_d and H are the exchange stiffness constant, Dzyaloshinskii–Moriya constant, magnetic permeability, saturation magnetization, demagnetizing field and external magnetic field. Material parameters used in the calculations correspond to the bulk FeGe material that hosts magnetic skyrmions at the nearly-room temperatures, which shows strong potential for technological applications. Energy terms are therefore set to $A = 4.75$ pJ/m, $D = 4\pi\frac{A}{\lambda} = 0.852$ mJ/m^2, with $\lambda = 70$ nm being helical length of the system and $M_s = 384$ kA/m while external magnetic field was 2000 G [34]. Dynamics under applied electrical current was examined through the Landau–Lifshitz–Gilbert equation [35] with the spin-transfer torque (STT) given as:

$$\frac{d\vec{m}}{dt} = -\gamma[\vec{m}\times\vec{H}_{eff} - (\vec{v}_e\cdot\nabla)\vec{m} + \alpha\vec{m}\times\frac{d\vec{m}}{dt} + \beta\vec{m}\times(\vec{v}_e\cdot\nabla)\vec{m}]. \quad (3)$$

where γ is the gyromagnetic ratio, $\vec{H}_{eff} = -\frac{1}{M_s}\frac{\delta E[\vec{m}]}{\delta\vec{m}}$ is effective magnetic field, α and β are Gilbert and non-adiabatic damping parameters. The drift velocity $\vec{v}_e = -[\frac{P\mu_B}{eM_S(1+\beta^2)}]\vec{j}_e$ is given by the polarization P, electron charge e and current density $\vec{j}_e$ [36]. Evaluating magnetization dynamics, Gilbert damping is set to 0.003 [37]. Non-adiabatic damping β was set to 0.3. Calculations were performed within Ubermag package with Mumax3 as a micromagnetic runner [38,39]. Cell discretization was set to 1 nm while time evolution was computed for 2 ns with 200 time steps.

3. Results and discussion

3.1. Skyrmion stabilization

The skyrmion diameter is affected by the underlying magnetic interactions, dominantly by the competition between the DMI and the isotropic Heisenberg exchange interaction. This competition can be related to the helical length, $\lambda = 4\pi\left|\frac{A}{D}\right|$ which is in our case equal to 70 nm. Dimensionality of the investigated nanorods and nanowires are laterally much smaller than 70 nm, resulting in a strong confinement of the skyrmion string. Initial magnetization was set to uniformly point in the positive z direction with a cylindrical defect (spanning along the whole thickness of the device) with magnetization pointing in $-z$ direction at the centre of the geometry. Such initial magnetization was then relaxed to obtain the magnetization configuration with minimal energy. To confirm that the obtained magnetization configuration is indeed a skyrmion string, the thickness-averaged topological charge was computed according to the Eq. (4):

$$Q = \frac{1}{N}\sum_{i=0}^{N} Q_i \quad (4)$$

where the summation goes over each magnetization slice along the length of the nanowire and nanorod, N denotes total number of slices in the model. For the present work we considered skyrmion tube as any configuration that satisfied $Q < -0.8$ and m_z magnetization component, along the skyrmion tube diagonal, exhibiting the antiparallel arrangement of magnetic moments in the centre and at the edge of the texture.

During the skyrmion relaxation, in the cases when $t < 50$ nm in both, the nanorods and nanowires with $w = 35$ nm and $d = 45$ nm, we observe a formation of the vortex state with $Q < -0.5$, rather than of magnetic skyrmion string with $Q \approx -1$. Such behaviour occurs due to a shift of skyrmion string phase in the magnetic phase diagram, where either a change of magnetic-field strength or a change in the material-specific energy terms would be required to stabilize the skyrmion string. Since in this study, we exclusively limit our focus to the geometric aspects of the 3D objects that may be considered in future applications, further investigation of the magnetic phase diagram is implemented. The cross-sections of relaxed magnetization configurations are presented in Fig. 2. It can be seen that the skyrmion-string-state stability is dominantly determined by the nanorod and nanowire length, and that in the cases presented in Fig. 2 the minimum length in 3D objects to stabilize skyrmion string is 50 nm when nanowire diameter and nanorod widths are 35 and 45 nm. The measured skyrmion string diameters for each geometry are listed in Table 1. The discrepancy in skyrmion size between the nanorod and nanowire occurs due to a demagnetizing field, which is larger in the case of nanorods leading to bigger skyrmion strings. [40,41]. Furthermore, the skyrmion string diameters are higher in the cases of shorter nanorods and nanowires.

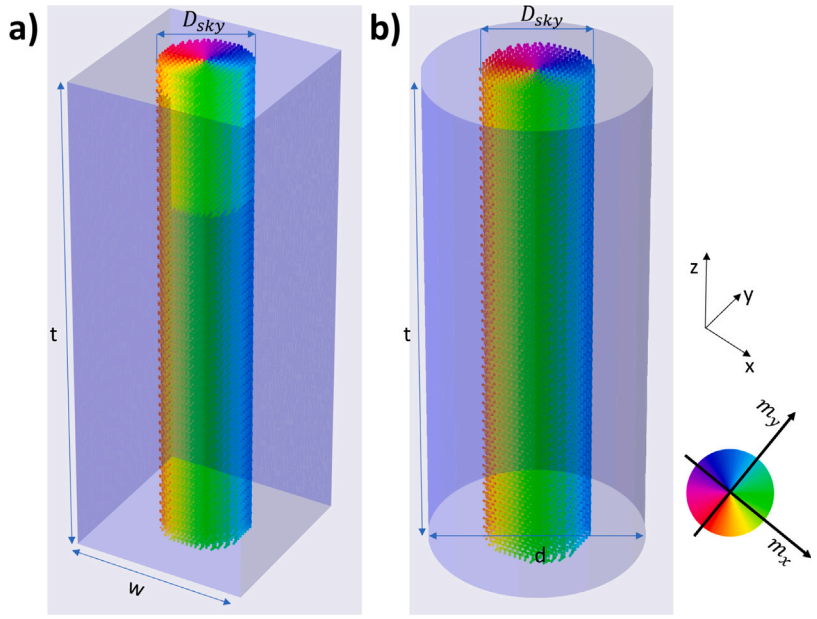

Fig. 1. Schematic representation of input models. (a) Nanorod and (b) nanowire with stabilized skyrmion string along the length of the object. The legend for the in-plane magentization directions is presented in top-down view where m_x and m_y are magnetization components in the x and y directions, respectively.

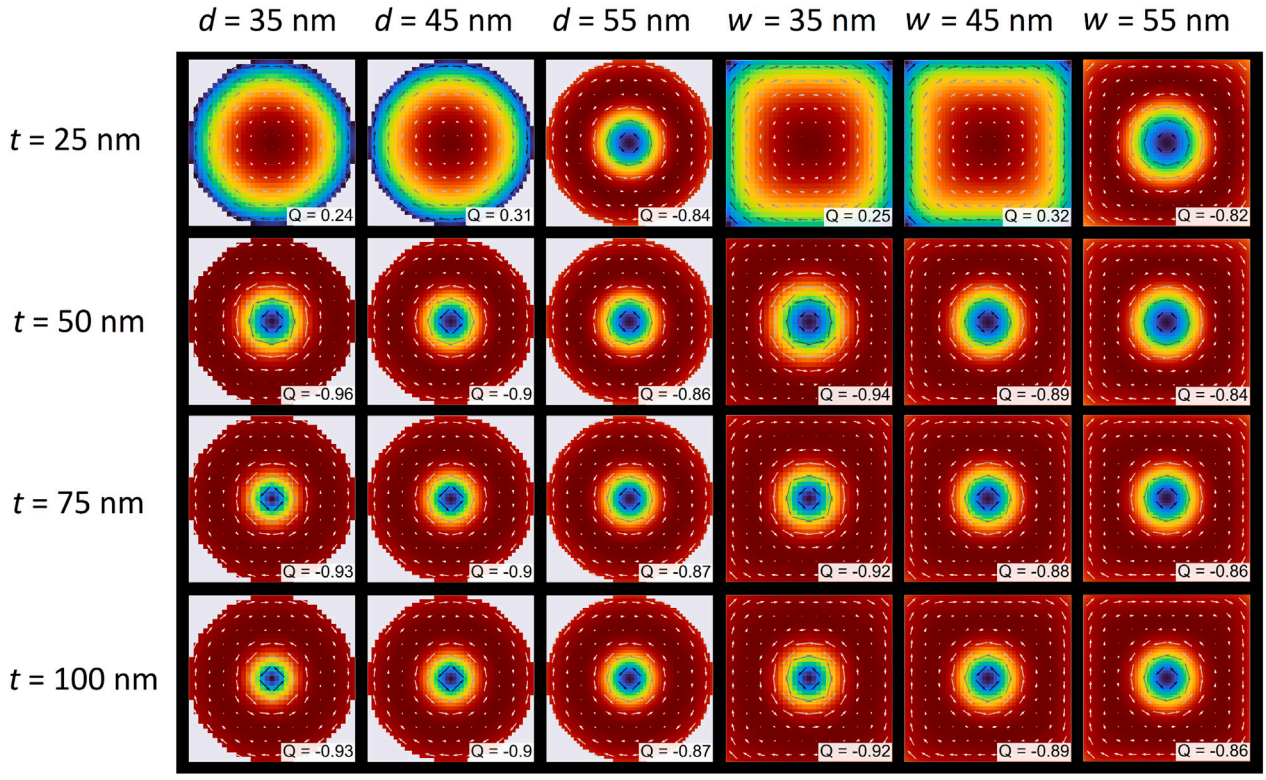

Fig. 2. Relaxed skyrmion string cross-sections with corresponding topological charges. Magnetization configurations of stabilized skyrmion strings are separated into columns where side width of nanorod and diameter of cylinder is kept constant, while along rows, length of the nanorods and nanowires is kept constant.

3.2. Current induced dynamics

After the magnetic-skyrmion strings have been stabilized, we apply an electrical current to the modelled objects and monitor the magnetization components and the time evolution of the topological charge. In the cases of a very small Gilbert damping, which is typical for bulk cubic chiral magnets like FeGe, the dominant term in Eq. (3) is related to precession. To increase the efficiency of the angular momentum transfer in affecting magnetization dynamics for miniaturized devices, three high values of the current densities are chosen: 1×10^{11}, 5×10^{11} and 1×10^{12} A/m^2 [42]. For small Gilbert damping ($\alpha = 0.003$) the magnetization dynamics is dominated by the precession term and the

Table 1
Measured diameters of stabilized skyrmion strings in calculated nanowires and nanorods.

	Nanowires			Nanorods		
	d = 35 nm	d = 45 nm	d = 55 nm	w = 35 nm	w = 45 nm	w = 55 nm
t = 25 nm	–	–	36.7 nm	–	–	42.8 nm
t = 50 nm	26.8 nm	30.7 nm	36.7 nm	30.1 nm	34.8 nm	40.7 nm
t = 75 nm	24.7 nm	30.7 nm	36.7 nm	26.8 nm	32.7 nm	38.7 nm
t = 100 nm	22.6 nm	28.6 nm	34.3 nm	26.8 nm	32.7 nm	38.7 nm

STT. Applied electrical currents are strong enough to de-pin skyrmion string and induce gyrotropic motion within the objects. For the object dimensions presented in this work, we observe skyrmion string motion without deformation along its length, which can be attributed to the confining effects of the modelled objects. As electrical current is switched on, we observe three distinct cases of the skyrmion string dynamics, (1) skyrmion string annihilation by at the edge of the nano-objects, (2) breathing and gyration of skyrmion string and (3) breathing and gyration coupled with topological charge unwinding. Due to geometrical confinement, skyrmion tube driven by the electrical current undergoes gyration, a circular motion within the cross-section of the nano-object. This motion arises from the interplay between the Magnus force and the confining boundaries, which prevents the skyrmion from moving freely along a straight path. In an ideal case, gyration can be utilized as skyrmion tube dynamic mode for frequency generation in STT based devices. Yet, the requirement for delicate balance between external drive and confining boundary repulsion is needed to prevent skyrmion string from annihilation. Despite the resiliency to continuous deformations implied by the topological character of skyrmion strings, the collision with the object walls can result in skyrmion string annihilation, provided that driving current is high enough to overcome repulsive force between skyrmion string and nano-object walls. Such annihilation is observed for nearly all shapes and sizes of nano-objects when applied current density was 1×10^{12} A/m^2 except for 50 nm long nanowire with 35 nm diameter where skyrmion string core gets pinned by the wall of the nano-objects allowing formation of half-skyrmion with approximately half-integer topological charge. For 5×10^{11} A/m^2 current density, skyrmion strings in nanowire exhibit significantly higher stability compared to their counterparts in nanorods. This higher stability can be attributed to the uniformity of dipolar field in the disc. Typically, the wall of the nano-object hosting a skyrmion string would act repulsively on a skyrmion string, but lack of the dipolar field uniformity in nanorods effectively reduces the repulsive force, resulting in a lower energy barrier for the skyrmion string annihilation. Additionally, as a skyrmion tube is driven by the current, a breathing mode is being triggered, increasing the skyrmion string diameter which results in skyrmion string edge colliding with the wall of the nano-object initiating topological charge unwinding. It has to be emphasized that a supposedly contradicting behaviour is observed for skyrmion-strings dynamics under 1×10^{11} A/m^2 drive, where a string in 35 nm wide and 50 nm long nanowire is preserved after 2 ns and a sting in 35 nm wide and 100 nm long nanowire is annihilated, while opposite occurs when applied current density is 1×10^{12} A/m^2. In our calculations electrical current was applied in the positive direction along the x-axis, therefore current-driven skyrmion annihilation will more likely occur if the skyrmion string is positioned next to the right edge of the nanowire, whereas a string positioned next to the left edge of the nanowire is more stable. This simply occurs due to the fact that the skyrmion motion is oriented in the same direction as the applied current, with the addition of the transverse motion due to Magnus force. On the other hand, due to a gyrotropic motion, at the instance of the skyrmion string-nanowire edge interaction, a skyrmion may be located on the opposing sides of the nanowire. Furthermore, the skyrmion-string speed is depends on the skyrmion string length, therefore, while driven by the current, the skyrmion string in 35 nm wide and 100 nm long nanowire, collides with nanowire wall leading to an annihilation. By applying a lower current density, 1×10^{11} A/m^2, skyrmion string is preserved both in nanowires and nanorods of all lengths and widths. In these cases, both gyrotropic motion and skyrmion string breathing cause local changes in magnetization that are periodic. To date, the skyrmion based STT oscillators utilizing either breathing or gyrotropic mode of frequency generation were already demonstrated. Among the studied nano-objects we identify that while 1×10^{11} A/m^2 of current density is applied, skyrmion strings can be used as STT oscillators. Further examining the complex interplay between gyrotropic motion, breathing dynamics and skyrmion string interactions with nanowire edges reveals that partial unwinding of the skyrmion string can serve as an additional mechanism for frequency generation. This is particularly visible in a 50 nm long nanowire with 35 nm width. In Fig. 3 we present the temporal evolution of the magnetization components and topological charge during the current-driven dynamics. The spectral analysis is performed on the mx(t), my(t), mz(t) and Q(t) signal and corresponding harmonics are marked. For harmonic detection, we used the prominence factor, a topographic measure to identify relevant harmonics relative to their background.

In the temporal evolution of measured mx, my, mz and Q, we see that oscillation modes are coupled as the dominant changes occur at the same moments in time, that is at 0.59 ns, 1.1 ns and 1.74 ns. The magnetization maps and corresponding topological charge density maps at these moments are shown in Fig. 4.

From the top panels of Fig. 4, depicting the magnetization maps, we can clearly see that the skyrmion-string cross-section lacks a defined radius due to the unwinding at the edges, since magnetic moments forming the skyrmion string located at the edge of the device are not twisting to lead towards unit topological charge.

The frequency spectra exhibit very strong fundamental oscillation at $f_0 = 0.503$ Ghz. Other harmonics are detected as multiples of the fundamental mode. The Table 2 contains harmonics extracted from the data. From Table 2 we can see that the oscillation modes are coupled, as most harmonics do not appear in single frequency spectra.

In frequency spectra of topological charge evolution, we identify a single harmonic positioned at the $f = 8.040$ GHz that is not present in any other signal; therefore, we assign it to be the mode of topological charge oscillation due to a partial skyrmion string unwinding. In Fig. 4, topological charge density maps, at the maxima of topological charge is asymmetric with enhanced weight towards the edge where the skyrmion string interacts weakly. The tail of the topological charge density is oriented towards the edge, where unwinding of the skyrmion string occurs. This indicates that a subsequent increase of the $Q(t)$ occurs due to the skyrmion-string interaction with the edge.

The pronounced amplitude variation of $Q(t)$ in the time domain, at $t = 1750$ ps can indicate the metastable oscillatory regime in which repeated oscillations can lead towards irreversible unwinding and annihilation of the skyrmion string. To prevent this outcome, a further stabilization mechanism may be required. For geometry as described here, in principle, an optical-vortex beam (OVB) might be utilized to create a stronger repulsive potential for the skyrmion string at the edge of the device [43,44]. The main advantage of using an OVB would be the possibility to tune the gyration radius, due to which the topological charge increase amplitude might stay fixed upon the breathing. Yet the applicability of the OVB would have to be investigated to appropriately tune the OVB frequency to maintain the sustained topological charge oscillation at constant amplitude and frequency.

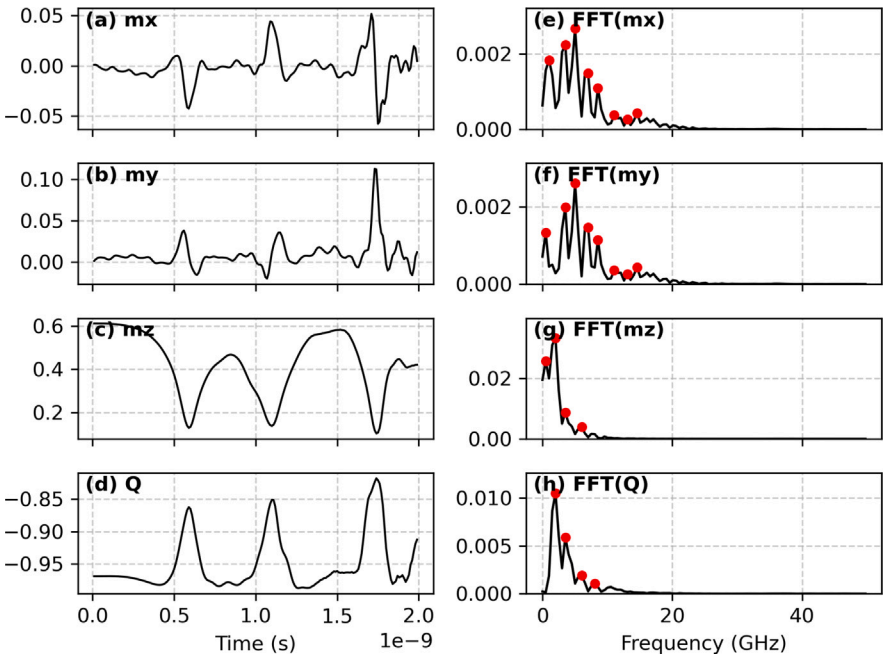

Fig. 3. (a)–(d) Temporal evolution of magnetization components and topological charge. (e)–(h) The Fourier transforms of components and topological charge. Harmonics detected by the prominence factor are marked with red circles.

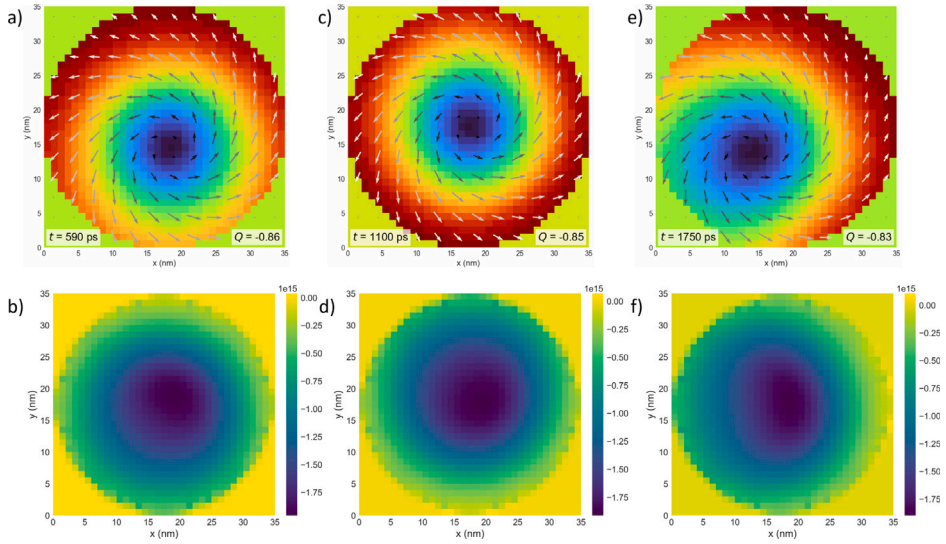

Fig. 4. Top row panels (a), (c), (e) show magnetization vector maps at time instances where extrema in $Q(t)$ are observed. The bottom row panels (b), (d) and (f) show corresponding topological charge density maps at the same time instances.

Table 2
Frequencies at which each observable exhibits peaks, expressed both in GHz and as integer multiples of the fundamental frequency $f_0 \approx 0.503$ GHz.

Observable	Frequencies (GHz)	Multiples of f_0
m_x	1.005, 3.518, 5.025, 7.035 8.543, 11.055, 13.065, 14.573	$2f_0,\ 7f_0,\ 10f_0,\ 14f_0$ $17f_0,\ 22f_0,\ 26f_0,\ 29f_0$
m_y	0.503, 3.518, 5.025, 7.035 8.543, 11.055, 13.065, 14.573	$f_0,\ 7f_0,\ 10f_0,\ 14f_0$ $17f_0,\ 22f_0,\ 26f_0,\ 29f_0$
m_z	0.503, 2.010, 3.518, 6.030	$f_0,\ 4f_0,\ 7f_0,\ 12f_0$
Q	2.010, 3.518, 6.030, 8.040	$4f_0,\ 7f_0,\ 12f_0,\ 16f_0$

From this analysis, we clearly identified that our frequency spectra was a result of dynamical mode mixing present in current-driven skyrmion string dynamics as indicated by the overlapping harmonics in Table 2, but single harmonic clearly indicates the independent mode at 8.04 GHz. Fig. 4 shows magnetization snippets, with corresponding topological charge densities showing where skyrmion string exhibits partial unwinding. The complete magnetization dynamics is provided as Supplementary video. Observed dynamics is a result of an appropriate parameter tuning, leading to partial and sustained oscillatory unwinding of the skyrmion string at the edge of the nanowire.

4. Conclusion

In this work, we have performed detailed analysis of the electrical-current-driven skyrmion string stability in a confined geometry. The role of geometric shape and material dimensions in dynamical behaviour is examined in detail by correlating temporal evolution of

the topological charge and by a visualization of the string dynamics. We show that specific nano-object geometries offer better performance, making them desirable for an application in spin-torque nano-oscillators. Furthermore, based on the behaviour of a topological charge for specific set of model parameter, we propose the idea of using topological charge oscillation as an additional mode of the frequency generation. Firstly, the applied current-density upper limit is determined to be 1×10^{11} A/m^2 where steady skyrmion string breathing and gyrotropic motion can be utilized for a frequency generation. Our results further show that current-induced drive of skyrmion string in confined geometry produces a non-trivial temporal evolution of topological charge along with the breathing dynamics and gyrotropic motion. We found that the nanowire geometry can be further utilized for design of STT nano-oscillators utilizing complex interplay of skyrmion string breathing dynamics, gyrotropic motion and interaction with the nanowire edges.

CRediT authorship contribution statement

Vinko Sršan: Writing – review & editing, Writing – original draft, Visualization, Methodology, Investigation, Formal analysis, Conceptualization. **Matej Komelj:** Writing – review & editing, Supervision, Project administration, Methodology, Investigation, Funding acquisition, Conceptualization. **Sašo Šturm:** Writing – review & editing, Supervision, Project administration, Methodology, Investigation, Funding acquisition, Conceptualization.

Declaration of competing interest

The authors declare that they have no known competing financial interests or personal relationships that could have appeared to influence the work reported in this paper.

Acknowledgements

This work has been funded by the Slovenian Research and Innovation Agency through P2-0084 research program and project J7-4637, European Union under the Horizon Europe Grant Agreement N° 101129888 as part of the GREENE project and by the Ministry of Higher Education, Science and Innovation of the Republic of Slovenia under grant agreement no. C3360–25–452010 (ERA-MIN project SIREN).

Appendix A. Supplementary data

Supplementary material related to this article can be found online at https://doi.org/10.1016/j.jmmm.2026.174171.

Data availability

Data will be made available on request.

References

[1] N. Nagaosa, Y. Tokura, Topological properties and dynamics of magnetic skyrmions, Nature Nanotechnology 8 (12) (2013) 899–911.
[2] U.K. Roessler, A. Bogdanov, C. Pfleiderer, Spontaneous skyrmion ground states in magnetic metals, Nature 442 (7104) (2006) 797–801.
[3] B. Binz, A. Vishwanath, V. Aji, Theory of the helical spin crystal: a candidate for the partially ordered state of MnSi, Phys. Rev. Lett. 96 (20) (2006) 207202.
[4] S. Mühlbauer, B. Binz, F. Jonietz, C. Pfleiderer, A. Rosch, A. Neubauer, R. Georgii, P. Böni, Skyrmion lattice in a chiral magnet, Science 323 (5916) (2009) 915–919.
[5] X. Yu, Y. Onose, N. Kanazawa, J.H. Park, J. Han, Y. Matsui, N. Nagaosa, Y. Tokura, Real-space observation of a two-dimensional skyrmion crystal, Nature 465 (7300) (2010) 901–904.
[6] A. Fert, P.M. Levy, Role of anisotropic exchange interactions in determining the properties of spin-glasses, Phys. Rev. Lett. 44 (23) (1980) 1538.
[7] C. Moreau-Luchaire, C. Moutafis, N. Reyren, J. Sampaio, C. Vaz, N. Van Horne, K. Bouzehouane, K. Garcia, C. Deranlot, P. Warnicke, et al., Additive interfacial chiral interaction in multilayers for stabilization of small individual skyrmions at room temperature, Nature Nanotechnology 11 (5) (2016) 444–448.
[8] O. Boulle, J. Vogel, H. Yang, S. Pizzini, D. de Souza Chaves, A. Locatelli, T.O. Menteş, A. Sala, L.D. Buda-Prejbeanu, O. Klein, et al., Room-temperature chiral magnetic skyrmions in ultrathin magnetic nanostructures, Nature Nanotechnology 11 (5) (2016) 449–454.
[9] S. Woo, K. Litzius, B. Krüger, M.-Y. Im, L. Caretta, K. Richter, M. Mann, A. Krone, R.M. Reeve, M. Weigand, et al., Observation of room-temperature magnetic skyrmions and their current-driven dynamics in ultrathin metallic ferromagnets, Nat. Mater. 15 (5) (2016) 501–506.
[10] P. Milde, D. Köhler, J. Seidel, L. Eng, A. Bauer, A. Chacon, J. Kindervater, S. Mühlbauer, C. Pfleiderer, S. Buhrandt, et al., Unwinding of a skyrmion lattice by magnetic monopoles, Science 340 (6136) (2013) 1076–1080.
[11] Y. Zhou, Magnetic skyrmions: intriguing physics and new spintronic device concepts, Natl. Sci. Rev. 6 (2) (2019) 210–212.
[12] X. Zhang, M. Ezawa, Y. Zhou, Magnetic skyrmion logic gates: conversion, duplication and merging of skyrmions, Sci. Rep. 5 (1) (2015) 1–8.
[13] R. Tomasello, E. Martinez, R. Zivieri, L. Torres, M. Carpentieri, G. Finocchio, A strategy for the design of skyrmion racetrack memories, Sci. Rep. 4 (1) (2014) 1–7.
[14] J. Sampaio, V. Cros, S. Rohart, A. Thiaville, A. Fert, Nucleation, stability and current-induced motion of isolated magnetic skyrmions in nanostructures, Nature Nanotechnology 8 (11) (2013) 839–844.
[15] H. Yang, C. Wang, X. Wang, X. Wang, Y. Cao, P. Yan, Twisted skyrmions at domain boundaries and the method of image skyrmions, Phys. Rev. B 98 (1) (2018) 014433.
[16] A. Fert, V. Cros, J. Sampaio, Skyrmions on the track, Nature Nanotechnology 8 (3) (2013) 152–156.
[17] W. Koshibae, N. Nagaosa, Dynamics of skyrmion in disordered chiral magnet of thin film form, Sci. Rep. 9 (1) (2019) 5111.
[18] W. Koshibae, N. Nagaosa, Bulk and surface topological indices for a skyrmion string: current-driven dynamics of skyrmion string in stepped samples, Sci. Rep. 10 (1) (2020) 20303.
[19] X. Yu, N. Nakanishi, Y.-L. Chiew, Y. Liu, K. Nakajima, N. Kanazawa, K. Karube, Y. Taguchi, N. Nagaosa, Y. Tokura, 3D skyrmion strings and their melting dynamics revealed via scalar-field electron tomography, Commun. Mater. 5 (1) (2024) 80.
[20] K. Ran, W. Tan, X. Sun, Y. Liu, R.M. Dalgliesh, N.-J. Steinke, G. van der Laan, S. Langridge, T. Hesjedal, S. Zhang, Bending skyrmion strings under two-dimensional thermal gradients, Nat. Commun. 15 (1) (2024) 4860.
[21] F. Zheng, F.N. Rybakov, N.S. Kiselev, D. Song, A. Kovács, H. Du, S. Blügel, R.E. Dunin-Borkowski, Magnetic skyrmion braids, Nat. Commun. 12 (1) (2021) 5316.
[22] J. Xia, X. Zhang, O.A. Tretiakov, H.T. Diep, J. Yang, G. Zhao, M. Ezawa, Y. Zhou, X. Liu, Bifurcation of a topological skyrmion string, Phys. Rev. B 105 (21) (2022) 214402.
[23] M.T. Birch, D. Cortés-Ortuño, N.D. Khanh, S. Seki, A. Štefančič, G. Balakrishnan, Y. Tokura, P.D. Hatton, Topological defect-mediated skyrmion annihilation in three dimensions, Commun. Phys. 4 (1) (2021) 175.
[24] S.I. Kiselev, J. Sankey, I. Krivorotov, N. Emley, R. Schoelkopf, R. Buhrman, D. Ralph, Microwave oscillations of a nanomagnet driven by a spin-polarized current, Nature 425 (6956) (2003) 380–383.
[25] A. Awad, P. Dürrenfeld, A. Houshang, M. Dvornik, E. Iacocca, R. Dumas, J. Åkerman, Long-range mutual synchronization of spin Hall nano-oscillators, Nat. Phys. 13 (3) (2017) 292–299.
[26] T.J. Silva, W.H. Rippard, Developments in nano-oscillators based upon spin-transfer point-contact devices, J. Magn. Magn. Mater. 320 (7) (2008) 1260–1271.
[27] A. Slavin, V. Tiberkevich, Nonlinear auto-oscillator theory of microwave generation by spin-polarized current, IEEE Trans. Magn. 45 (4) (2009) 1875–1918.
[28] X. Liang, L. Shen, X. Xing, Y. Zhou, Elongated skyrmion as spin torque nano-oscillator and magnonic waveguide, Commun. Phys. 5 (1) (2022) 310.
[29] F. Garcia-Sanchez, J. Sampaio, N. Reyren, V. Cros, J. Kim, A skyrmion-based spin-torque nano-oscillator, New J. Phys. 18 (7) (2016) 075011.
[30] S. Zhang, J. Wang, Q. Zheng, Q. Zhu, X. Liu, S. Chen, C. Jin, Q. Liu, C. Jia, D. Xue, Current-induced magnetic skyrmions oscillator, New J. Phys. 17 (2) (2015) 023061.
[31] J.-V. Kim, F. Garcia-Sanchez, J. Sampaio, C. Moreau-Luchaire, V. Cros, A. Fert, Breathing modes of confined skyrmions in ultrathin magnetic dots, Phys. Rev. B 90 (6) (2014) 064410.
[32] R. Xing, Y. Kou, Y. Wang, J. Zhou, Y. Wei, L. You, R. Xiong, Z. Zeng, S. Liang, X. Yang, et al., Strong skyrmion oscillations driven by spatially dependent spin current, Phys. Rev. Appl. 13 (5) (2020) 054055.
[33] X. Yu, N. Kanazawa, Y. Onose, K. Kimoto, W. Zhang, S. Ishiwata, Y. Matsui, Y. Tokura, Near room-temperature formation of a skyrmion crystal in thin-films of the helimagnet FeGe, Nat. Mater. 10 (2) (2011) 106–109.
[34] F. Zheng, N.S. Kiselev, F.N. Rybakov, L. Yang, W. Shi, S. Blügel, R.E. Dunin-Borkowski, Hopfion rings in a cubic chiral magnet, Nature 623 (7988) (2023) 718–723.

[35] T.L. Gilbert, A phenomenological theory of damping in ferromagnetic materials, IEEE Trans. Magn. 40 (6) (2004) 3443–3449.
[36] S. Zhang, Z. Li, Roles of nonequilibrium conduction electrons on the magnetization dynamics of ferromagnets, Phys. Rev. Lett. 93 (2004) 127204.
[37] S. Budhathoki, A. Sapkota, K.M. Law, S. Ranjit, G.M. Stephen, D. Heiman, M.E. Jamer, T. Mewes, A.J. Hauser, Ultralow effective Gilbert damping and induced orbital moment in strain-engineered FeGe films with Curie temperature exceeding room temperature, J. Magn. Magn. Mater. 564 (2022) 170053.
[38] M. Beg, M. Lang, H. Fangohr, Ubermag: Towards more effective micromagnetic workflows, IEEE Trans. Magn. 58 (2) (2022) 1–5.
[39] A. Vansteenkiste, J. Leliaert, M. Dvornik, M. Helsen, F. Garcia-Sanchez, B. Van Waeyenberge, The design and verification of MuMax3, AIP Adv. 4 (10) (2014).
[40] H. Vigo-Cotrina, A. Guimarães, Influence of the dipolar interaction in the creation of skyrmions in coupled nanodisks, J. Magn. Magn. Mater. 489 (2019) 165406.
[41] H. Kwon, K. Bu, Y. Wu, C. Won, Effect of anisotropy and dipole interaction on long-range order magnetic structures generated by Dzyaloshinskii–Moriya interaction, J. Magn. Magn. Mater. 324 (13) (2012) 2171–2176.
[42] M.D. Stiles, J. Miltat, Spin-transfer torque and dynamics, Spin Dyn. Confin. Magn. Struct. III (2006) 225–308.
[43] S. Guan, Y. Liu, Z. Hou, D. Chen, Z. Fan, M. Zeng, X. Lu, X. Gao, M. Qin, J.-M. Liu, Optically controlled ultrafast dynamics of skyrmion in antiferromagnets, Phys. Rev. B 107 (21) (2023) 214429.
[44] Y. Lei, Q. Yang, Z. Tang, G. Tian, Z. Hou, M. Qin, Rotational motion of skyrmion driven by optical vortex in frustrated magnets, Appl. Phys. Lett. 125 (7) (2024).